

Supporting information

Regulating crystallization dynamics and crystal orientation of methylammonium tin iodide enables high-efficiency lead-free perovskite solar cells

Long Ji,^{a,b} Ting Zhang,^{a*} Yafei Wang,^a Detao Liu,^a Hao Chen,^a Hualin Zheng,^a Xuefeng Peng,^a

Shihao Yuan,^a Zhi David Chen,^c Shibin Li,^{a,d*}

^aSchool of Optoelectronic Science and Engineering, University of Electronic Science and Technology of China (UESTC), Chengdu, Sichuan 610054, China

^bLaboratory of Photonics and Interfaces, Institute of Chemical Sciences and Engineering, École Polytechnique Fédérale de Lausanne (EPFL), Lausanne, Switzerland.

^cDepartment of Electrical & Computer Engineering and Center for Nanoscale Science & Engineering, University of Kentucky, Lexington, Kentucky 40506, USA

^dYangtze Delta Region Institute (Huzhou) , University of Electronic Science and Technology of China, Huzhou 313001, P. R. China

*Corresponding author. E-mail: shibinli@uestc.edu.cn; tzhang@uestc.edu.cn

Experimental Section

Materials: MAI (99.99%), EABr (99.99%), EDAl₂ (99.99%), BCP, PEDOT:PSS were purchased from Xi'an p-OLED Corp. PC₆₁BM, ITO (substrate, sheet resistance is 15 Ω sq⁻¹) and chlorobenzene were purchased from YouXuan. SnI₂ (99.99%) and dimethylsulfoxide (DMSO) were purchased from Sigma-Aldrich.

Film Preparation: The preparation of the precursor solution was prepared by mixing (0.98-x)M MAI, xM EABr, 1M SnI₂, 1%M EDAl₂, 0.1M SnF₂ in DMSO. The MASnI_{3-x} EABr perovskite precursor solutions with EABr in varied proportions were prepared on maintaining the SnI₂, SnF₂ and EDAl₂ concentration same as the standard condition and altering the molar ration EABr:MAI. MASnI_{3-x} EABr with varied x - 0%, 10%, 20%, 30%, 40%, 50%, 60%, 70%. All of these preparations were done in a glove box.

Device Fabrication: ITO glass substrates were cleaned by sequential ultrasonication in acetone, ethanol, and deionized water for 15 min each. Then the cleaned ITO was treated with ultraviolet-ozone for 15 min before device fabrication. The PEDOT:PSS aqueous solution was filtered by a 0.45 μm filter before use, then the PEDOT:PSS solution was spin-coated on the cleaned ITO substrates at 5000 rpm for 40 s, and then annealed at 150 °C for 20 min in ambient. The perovskite precursor solution of MASnI_{3-x} EABr with different x values (0%, 10%, 20%, 30%, 40%, 50%, 60%, 70%) were deposited on PEDOT:PSS coated ITO substrates and spin-coated at 1000 rpm for 10 s and then 5000 rpm for 40 s in a glove box. 0.3ml anti-solvent of chlorobenzene was dropped onto the spinning substrates during the spin-coating and

then the samples were annealed at 70 °C for 10 min. Then, PC₆₁BM solution (20 mg ml⁻¹ in chlorobenzene) and BCP (0.5 mg/ml in isopropyl alcohol) was deposited subsequently at 2000 rpm for 30 s and 3000 rpm for 30 s, respectively. Finally, a 90 nm thickness of Ag electrode was evaporated under high vacuum ($<1\times 10^{-6}$ Torr).

Characterization: GIWAXS was performed at the Shanghai Synchrotron Radiation Facility (SSRF), Zhangjiang Lab., with incident angle of 2°. X-ray diffraction (XRD) measurements were carried out using a Bede D1 system with Cu K α radiation. SEM was measured by a field emission fitting SEM (FEI-Inspect F50, Holland). The UV-vis absorption spectrum was measured by an ultraviolet-visible (UV-vis) spectrophotometer (Schimadzu UV-3101 PC). *J-V* curves were measured in the air using Keithley 2400 Source Meter under 100 mW cm⁻² AM 1.5 G solar irradiation. XPS was measured using the Kratos XSAM 800 X-Ray Photoelectron Spectrometer. The time-resolved photoluminescence (TRPL) spectra of the samples were measured using a Fluorolog-3 fluorescence spectrophotometer, a 510 nm laser was employed as the excitation light, and double-exponential decay model was used to fit the PL decay. The EIS measurements were performed using electrochemical workstation (chi660d). The applied voltage perturbation had an AC amplitude of 10 mV (rms) under darkness at 0.3 V with a frequency from 100 mHz – 4 MHz. The impedance parameters were simulated by fitting of the impedance spectra using Zview software. Capacitance-voltage (C-V) measurements were conducted on applying a perturbation 10 mV of AC voltage at frequency 1 kHz, which was superimposed on the DC bias to yield the final C-V curves.

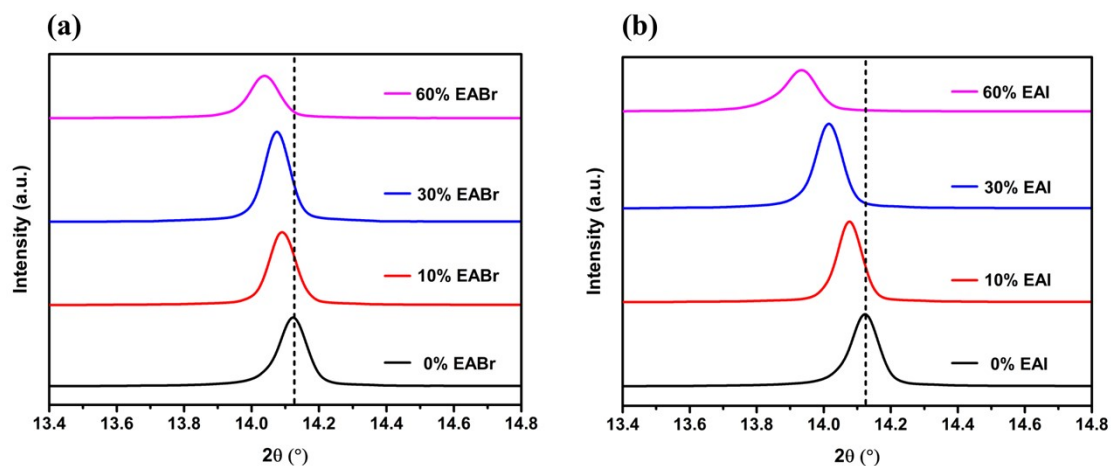


Figure S1. (a) Magnified XRD patterns of (100) peak of MASnI_3 perovskite with 0 mol%, 10 mol%, 30 mol%, 60 mol% EABr addition. (b) Magnified XRD patterns of (100) peak of MASnI_3 perovskite with 0 mol%, 10 mol%, 30 mol%, 60 mol% EAI addition.

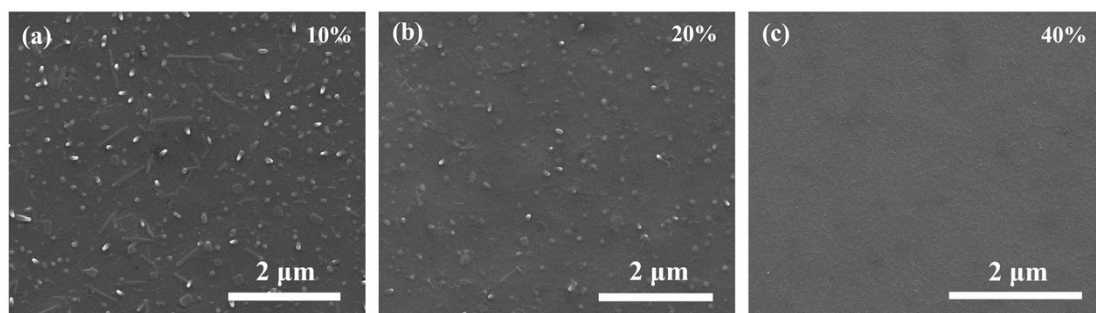


Figure S2. (a)-(c) SEM images of MASnI_{3-x} EABr ($x=10$ mol%, 20 mol%, 40 mol%) perovskite films.

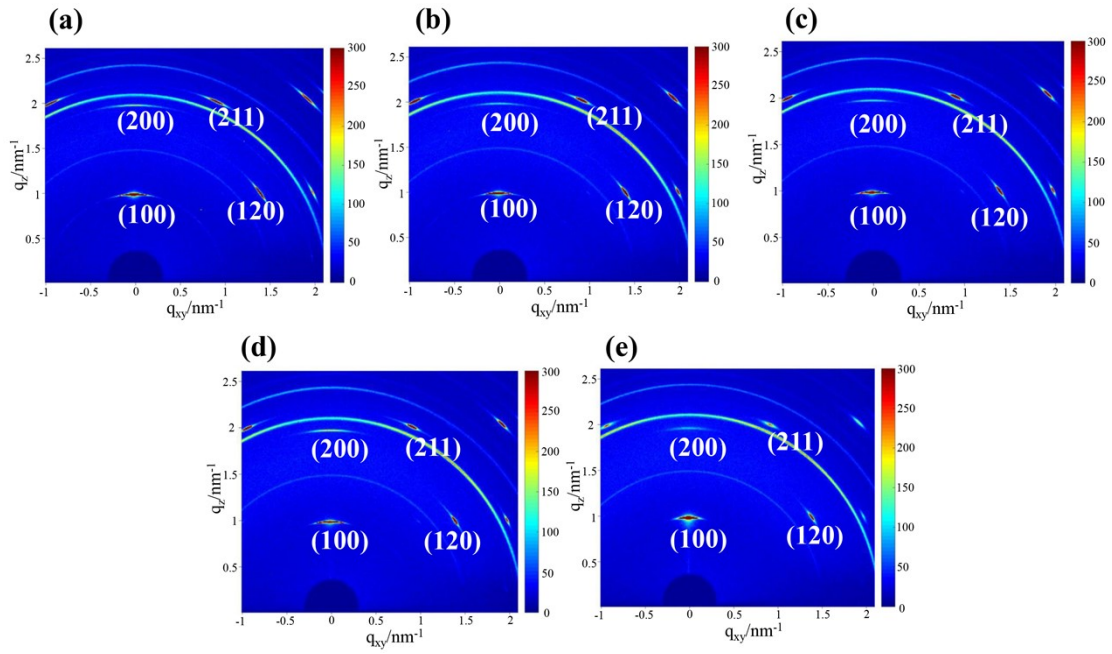


Figure S3. (a)-(e) GIWAXS patterns of $\text{MASnI}_{3-x}\text{EABr}$ ($x=10, 20, 40, 50, 70$ mol%) perovskite films.

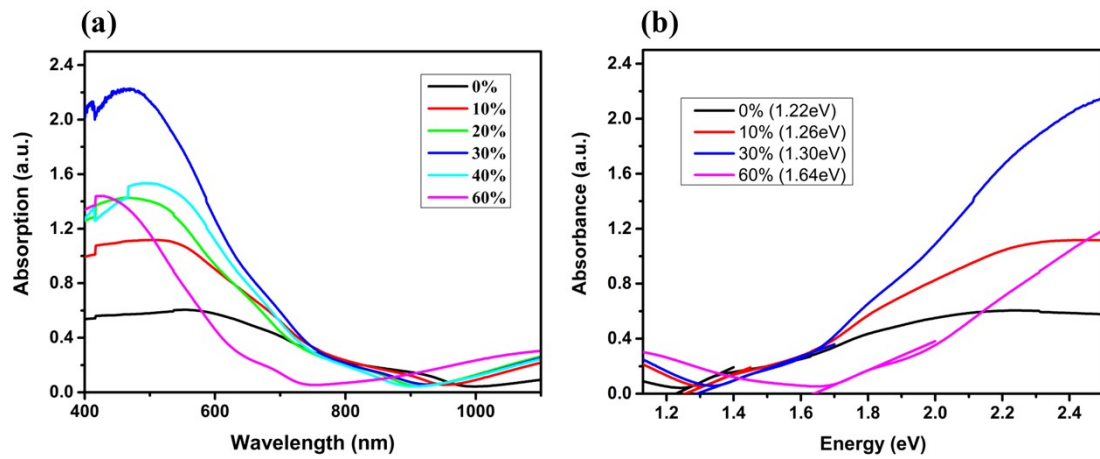


Figure S4. (a) UV-vis spectra of $\text{MASnI}_{3-x}\text{EABr}$ ($x=0$ mol%, 10 mol%, 20 mol%, 30 mol%, 40 mol%, 60 mol%) perovskite film. (b) Absorption spectra of $\text{MASnI}_{3-x}\text{EABr}$ ($x=0$ mol%, 10 mol%, 30 mol%, 60 mol%) perovskite film.

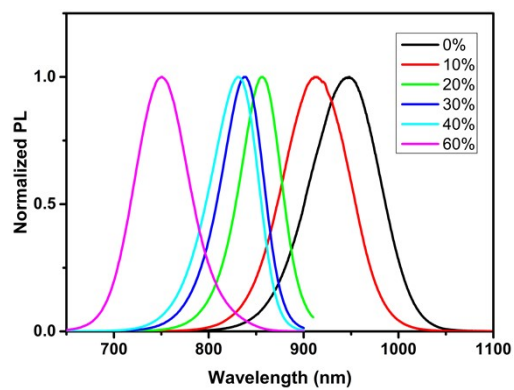


Figure S5. Normalized PL spectra of MASnI_{3-x} EABr ($x = 0 \text{ mol\%}$, 10 mol\% , 20 mol\% , 30 mol\% , 40 mol\% , 60 mol\%) perovskite film.

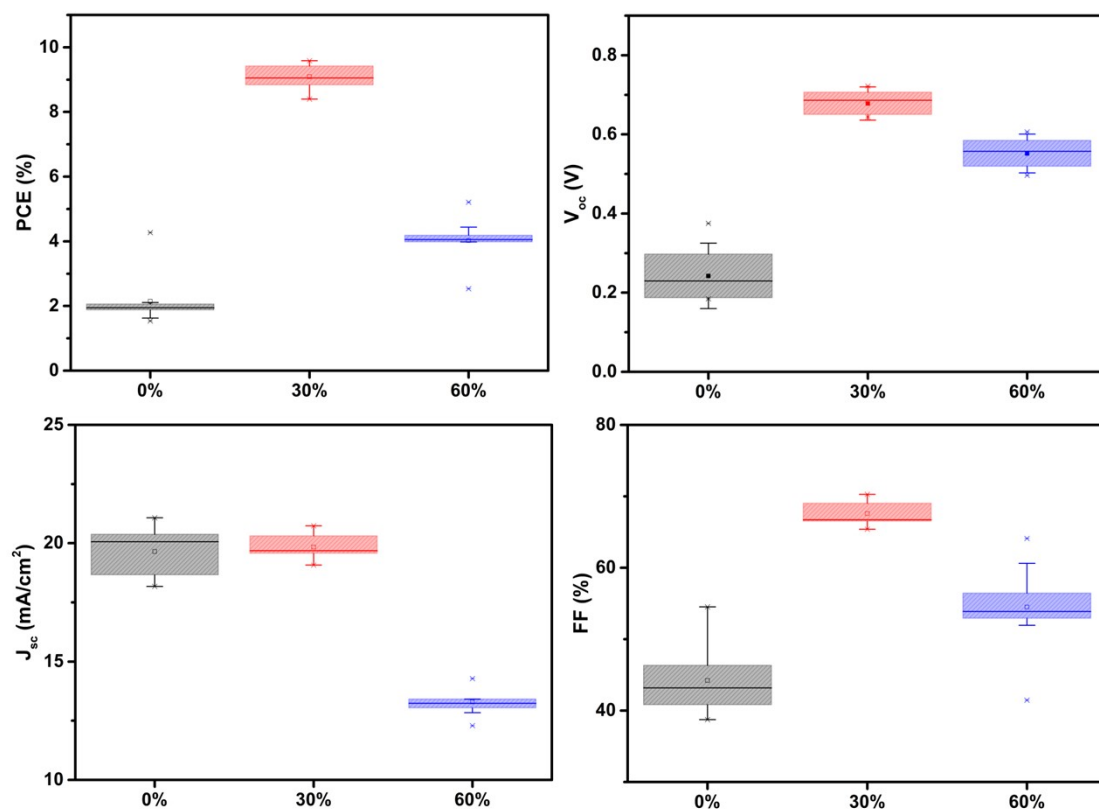


Figure S6. Photovoltaic parameters of 9 cells based on MASnI_{3-x} EABr ($x = 0 \text{ mol\%}$, 30 mol\% , 60 mol\%) perovskite films fabricated under the same experimental conditions.

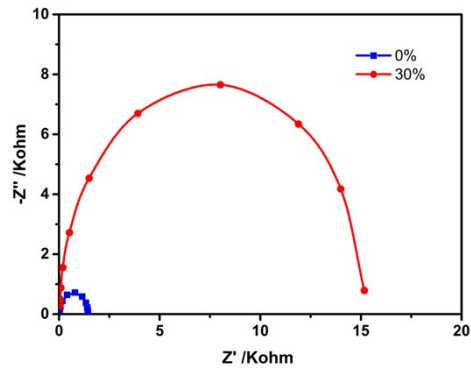


Figure S7. Nyquist plots of the EIS measurement of MASnI_{3-x} EABr ($x=0$ mol%, 30 mol%) perovskite device.

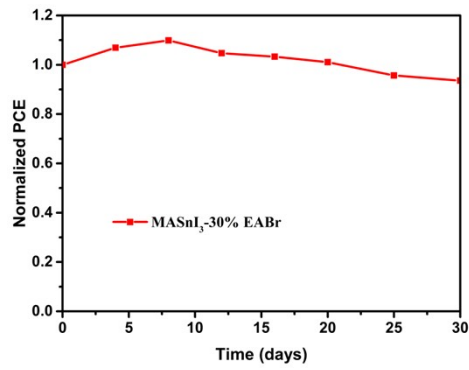


Figure S8. Stability measurement of our champion cell.

Table S1. Crystallographic data of MASnI_{3-x} EABr (x=0 mol%, 30 mol%, 60 mol%) and MASnI_{3-x} EAI (x= 30 mol%, 60 mol%) perovskite films.

| Compound | MASnI ₃ -0% EABr | MASnI ₃ -30% EABr | MASnI ₃ -60% EABr | MASnI ₃ -30% EAI | MASnI ₃ -60% EAI |
|--------------------------|-----------------------------|------------------------------|------------------------------|-----------------------------|-----------------------------|
| Lattice structure | cubic | cubic | cubic | cubic | cubic |
| Miller indices (hkl) | (100) | (100) | (100) | (100) | (100) |
| Lattice constant (a=b=c) | 3.1605 Å | 3.1649 Å | 3.1779 Å | 3.1819 Å | 3.2005 Å |

Table S2. Time coefficients (relative amplitudes in parentheses) derived from fitting the PL transients of the corresponding perovskite films from a double-exponential fit

$$\tau_{\text{ave}} = \frac{A_1\tau_1^2 + A_2\tau_2^2}{A_1\tau_1 + A_2\tau_2}$$

(Figure 4b), the calculation formula of $\tau_{\text{ave}} = \frac{A_1\tau_1^2 + A_2\tau_2^2}{A_1\tau_1 + A_2\tau_2}$.

| MASnI _{3-x} EABr | τ_1 /ns(A ₁) | τ_2 /ns(A ₂) | τ_{ave} /ns |
|---------------------------|-------------------------------|-------------------------------|-------------------------|
| 0% | 1.34 (0.14) | 0.21 (0.97) | 0.74 |
| 30% | 1.09 (1.02) | 3.84 (0.04) | 1.43 |

Table S3. Photovoltaic parameters of the champion PSCs based on the MASnI_{3-x} EABr (x=0 mol%, 10 mol%, 30 mol%, 60 mol%) under forward scan.

| x | V _{oc} (V) | J _{sc} (mA/cm ²) | FF (%) | PCE (%) |
|-----|---------------------|---------------------------------------|--------|---------|
| 0% | 0.38 | 20.88 | 54.51 | 4.27 |
| 10% | 0.53 | 20.13 | 57.60 | 6.19 |
| 30% | 0.72 | 19.08 | 69.62 | 9.59 |
| 60% | 0.60 | 12.66 | 65.54 | 4.98 |

